

Dimers at Ge/Si(001) surfaces: Ge coverage dependent quenching, reactivation of flip-flop motion, and interaction with dimer vacancy lines

H. Hirayama,* H. Mizuno, and R. Yoshida

Department of Materials Science and Engineering, Tokyo Institute of Technology 4259 Nagatsuda, Midori-ku, Yokohama 226-8502, Japan

(Received 10 May 2002; published 29 October 2002)

We studied Ge coverage (θ_{Ge}) dependent quenching, reactivation of the flip-flop motion, and interaction with dimer vacancy lines (DVLs) of dimers on Ge/Si(001) surfaces using a scanning tunneling microscope (STM) combined with a molecular beam epitaxy apparatus. Deposition of ~ 0.3 ML (monolayer) Ge quenched the flip-flop motion, making all dimers asymmetric. Further deposition introduced DVLs at $\theta_{Ge} \geq \sim 0.5$ ML, and symmetric dimer domains appeared again locally at $\theta \geq 1.5$ ML. High-resolution STM images indicated that asymmetric dimer rows always invert their phase in alternation with buckled dimer's up-end at the DVLs. Low-temperature STM images indicated that the symmetric dimer domains were due to flip-flopping of asymmetric dimers activated by large θ_{Ge} at room temperature. The symmetric dimer domains extended along the dimer rows over the DVLs due to the phase correlation.

DOI: 10.1103/PhysRevB.66.165428

PACS number(s): 68.35.Bs, 68.37.Ef, 68.55.-a, 81.15.Hi

I. INTRODUCTION

The Si(001) surface is intrinsically a 2×1 reconstruction with symmetric dimer rows at room temperature,^{1,2} though C-type defects and steps induce buckling extrinsically and make the adjacent dimers asymmetric.³⁻⁵ Theoretical calculations indicate that an asymmetric dimer structure is energetically more stable than a symmetric dimer structure.⁶ Scanning tunneling microscope (STM) and low-energy electron diffraction (LEED) studies at low temperature^{7,8} revealed that the 2×1 reconstruction of the Si(001) surface is due to a flip-flop motion of the asymmetric dimers activated at room temperature.

In contrast to Si(001) surfaces, local $c(2 \times 4)$ and $p(2 \times 2)$ orderings with asymmetric dimers are dominant on Ge(001) surfaces at room temperature.⁹ The asymmetric dimers are intrinsic and do not require defects on Ge(001) surfaces to be quenched because the dimer buckling is energetically more stable than on Si(001) surfaces.¹⁰ However, Zandvliet *et al.* reported recently that $c(2 \times 4)$ asymmetric and 2×1 symmetric dimer domains appeared alternately at the surface with very low (0.15%) defect density.¹¹ The alternation was attributed to cancellation of the anisotropic strain energy of the two domains.

The change of the surface structure with Ge deposition on an Si(001) surface is of great interest. Two-dimensional wetting Ge layers several monolayers (ML) thick were initially formed due to a 4% lattice mismatch. Three-dimensional Ge islands subsequently grew during Ge growth on the Si surfaces.¹²⁻¹⁴ $2 \times N$ reconstruction with dimer vacancy lines (DVLs) perpendicular to the dimer rows appears to release Ge-induced surface stress in the initial two-dimensional wetting layer growth.¹⁵⁻¹⁷ The stress also causes reversal of the S_A and S_B step roughness^{18,19} and the appearance of the energetically unfavorable D_A step at the Ge/Si(001) surfaces.²⁰ However, the Ge coverage (θ_{Ge}) dependent change from symmetric to asymmetric dimers and their interaction with the DVLs were not studied in detail, though asymmetric dimers were widely observed on the Ge/Si(001) surfaces of

fixed coverages.^{15,16,18-22} We addressed these points in this study using STM. The symmetric dimers were completely changed to asymmetric dimers by a small amount of Ge deposition of $\theta_{Ge} \leq 0.3$ ML, as described below. However, symmetric dimer domains reappeared at $\theta_{Ge} \geq \sim 1.5$ ML. The DVLs function as a phase inverter in the alternation of up-end atoms in the asymmetric dimer rows.

II. EXPERIMENT

Experiments were performed in an ultrahigh-vacuum apparatus consisting of a loading chamber, a sample preparation chamber, a molecular beam epitaxy (MBE) chamber, and a main chamber equipped with an STM unit (Unisoku USM-1200). The base pressure of the MBE chamber was 3×10^{-8} Pa and that of the preparation and main chambers was 1×10^{-8} Pa. The $2 \times 10 \times 0.4$ mm³ samples were cut from mirror-polished commercial Si(001) wafers. They were preheated in the preparation chamber at 500 °C overnight. The samples were then flashed at 1200 °C and slowly cooled to room temperature. We confirmed the surface cleanliness by STM so that we could observe the 2×1 reconstruction.

A sample was transferred to the MBE chamber after cleaning. Ge was deposited from a commercial Knudsen cell. The Ge growth rate was determined prior to this study by cross-sectional field emission secondary electron microscope (FE-SEM) observation of Ge films grown on SiO₂ surfaces. The growth rate was estimated from the linear relationship between the Ge film thickness and deposition time. Ge was deposited on the Si(001) substrates at a growth rate of 0.056 ML (monolayer)/sec in this study. The Ge Knudsen cell was kept at a constant temperature during the experiment by a computer-controlled feedback system. The Ge cell shutter was opened first in the deposition. The main shutter was opened after the Ge flux was confirmed to be at a preset value, and Ge was deposited on the substrate. Ge coverage was controlled by the deposition time. The substrate temperature was kept at 680 °C during the deposition. The structure of the sample surface was observed by STM at room temperature for every small increase of Ge coverage. The

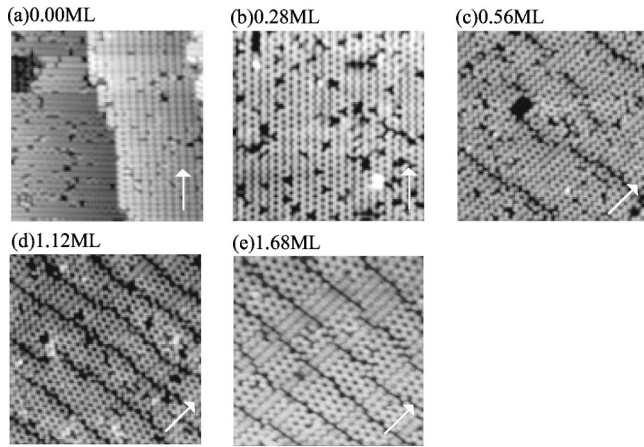


FIG. 1. STM images of Ge/Si(001) surfaces. Ge was deposited at 680 °C. Images were taken at room temperature. (a) $\theta_{Ge} = 0$ ML, (b) $\theta_{Ge} = 0.28$ ML, (c) $\theta_{Ge} = 0.56$ ML, (d) $\theta_{Ge} = 1.12$ ML, and (e) $\theta_{Ge} = 1.68$ ML. 20×20 nm². $V_s = -2.0$ V, $I_t = 0.25$ A. Arrows indicate the $\{110\}$ direction.

sample surface was also observed by STM at liquid N₂ temperature at $\theta_{Ge} = 1.68$ ML. STM images were obtained with a sample bias voltage of -2.0 V and a tunneling current of 0.25 nA. Images are shown with a conventional gray scale keyed to the surface height.

III. RESULTS

Figure 1 shows a series of STM images taken at room temperature with small increases of Ge coverage. The image size was 20×20 nm². Arrows in the figure indicate the $\{110\}$ direction on the surface. The Ge coverage was (a) 0, (b) 0.28, (c) 0.56, (d) 1.12, and (e) 1.68 ML. The surface exhibited the intrinsic 2×1 reconstruction of a Si(001) surface at 0 ML coverage [Fig. 1(a)]. Dimers were imaged as symmetric beans over most of the surfaces. The dimers were asymmetric only at the step edges and near C-type defects where anisotropic strain was introduced to adjacent dimers. Their alternation of the up-end made the dimer rows appear as zigzag chains.^{3,4,23}

The symmetric dimers disappeared with 0.28 ML Ge deposition, and zigzag chains of alternating asymmetric dimers appeared everywhere [Fig. 1(b)]. Symmetric dimers completely changed to asymmetric dimers when a small amount of Ge was added. The zigzag chains extended independently of the defects even though the surface included many defects. The out-of-phase and in-phase alignments of adjacent zigzag dimer rows caused $c(2 \times 4)$ and $p(2 \times 2)$ local ordering at the surface.^{10,22-24} The proportions of $c(2 \times 4)$ and $p(2 \times 2)$ local domains were almost even at $\theta_{Ge} = 0.28$ ML.

The surface was still covered by asymmetric dimers at $\theta_{Ge} = 0.56$ ML [Fig. 1(c)], but new DVLs were introduced to the surface [dark lines perpendicular to the zigzag chains of the asymmetric dimer rows in Fig. 1(c)]. The DVLs extended in almost straight lines perpendicular to the dimer rows, introducing $2 \times N$ ordering at the surface. The average distance

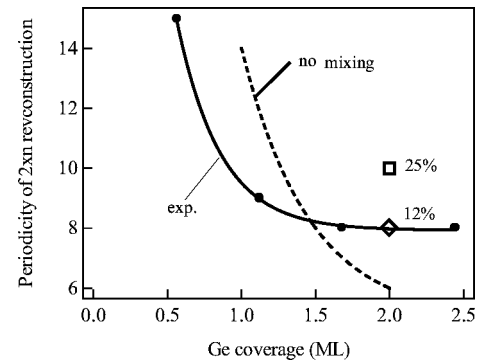


FIG. 2. θ_{Ge} vs DVL distance N . Dots: experiments. Dashed line: calculated value with no intermixing. Square and diamond: calculated values for 25% and 12% intermixing cases. Solid line is a visual guide.

between DVLs (N) was $15a$ (a is the atomic distance of the 1×1 surface unit cell).

The surface took on $c(2 \times 4)$ local ordering over almost all the area at $\theta_{Ge} = 1.12$ ML [Fig. 1(d)], and N decreased to $\sim 9a$. Here N became constant at $\sim 8a$ with further deposition [$\theta_{Ge} = 1.68$ ML Fig. 1(e)]. The θ_{Ge} -dependent change of N is indicated by dots in Fig. 2.

Symmetric dimer rows reappeared locally at the surface at $\theta_{Ge} = 1.68$ ML. The symmetric dimer domains were characteristic in extending along the dimer row direction over the DVLs and occupied $\sim 20\%$ of the total area. These 2×1 local domains disappeared at liquid N₂ temperature, as shown in Fig. 3.

A high-resolution STM image of the surface of $\theta_{Ge} = 1.12$ ML is shown in Fig. 4(a). Bright protrusions correspond to the upper atoms of the asymmetric dimers in our occupied state STM, as discussed in the next section. The figure indicates that the upper atoms of the asymmetric dimer in the upper domain were aligned so as to never face the upper atoms of the asymmetric dimers in a lower domain at the DVL. This caused a phase inversion in the alternating up-end atoms in asymmetric dimer rows at the DVLs.

IV. DISCUSSION

The complete change from symmetric to asymmetric dimers caused by a small amount of Ge deposition is consistent with previous studies. The surface in a previous STM

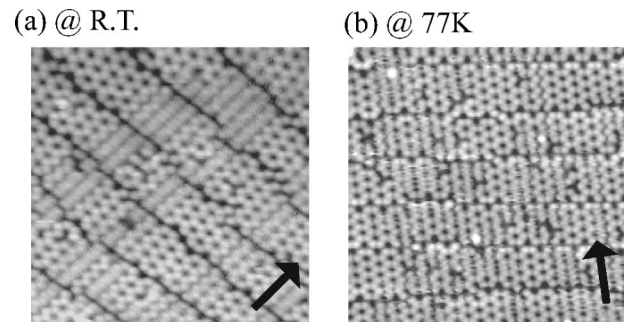


FIG. 3. STM images of the Ge/Si(001) surface at $\theta_{Ge} = 1.68$ ML taken at (a) room temperature and (b) liquid N₂ temperature. Arrows indicate the $\{110\}$ direction.

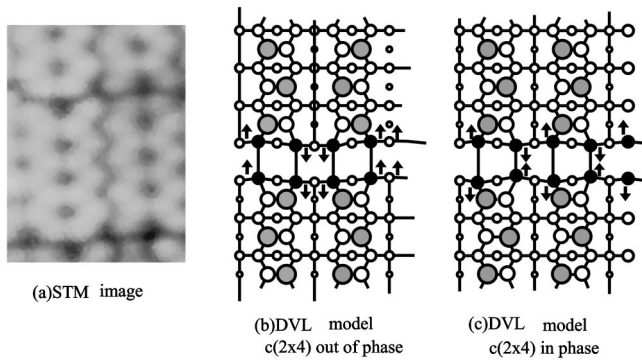


FIG. 4. High-resolution STM image of the Ge/Si(001) surface at $\theta_{Ge} = 1.12$ ML (a) and ball-and-stick models of the surface where the zigzag chains of the upper and lower domains are (b) out of phase and (c) in phase at DVL.

image of a 0.1 ML Ge/Si(001) surface was covered by asymmetric dimers.²⁴ A photoelectron diffraction study²⁵ also concluded that the Si(001) surface with 0.1 ML Ge assumes an asymmetric dimer structure. Both the present and previous studies indicate that the symmetric dimers were completely changed to asymmetric dimers by deposition of a very small amount of Ge ($\theta_{Ge} = 0.1-0.3$ ML).

A photoelectron diffraction study²⁵ demonstrated that Ge atoms take substitutional sites and form Ge-up/Si-down asymmetric mixed dimers at $\theta_{Ge} = 0.1$ ML. This Ge-Si mixed dimer should also form at the Ge-adsorbed sites of our $\theta_{Ge} = 0.28$ ML surface. However, 0.28 ML Ge did not cover all the surface sites. Thus, Si-Si and Si-Ge dimers coexisted at the surface. A small number of Ge-Si asymmetric mixed dimers seemed to halt the flip-flop motion of the remaining Si-Si dimers, making them asymmetric also. Theoretical calculations indicated that both Si-Ge and Si-Si asymmetric dimers concentrate the occupied state charge distribution on the up atoms.^{6,10,26,27} Thus, alternation of up-end atoms of Ge-Ge and Si-Si asymmetric dimers was observed as zigzag chains in our occupied state STM image, in which Ge-Si and Si-Si dimers could not be distinguished.

The Ge-Si dimer assumes a Ge-up/Si-down asymmetric structure because of its large energy gain. First-principles theoretical calculations on the Ge/Si(001) surface of $\theta_{Ge} = 0.5$ ML (Ref. 26 and 27) indicated that the Ge-up/Si-down asymmetric dimer is 0.55 eV more energetically favorable than the Ge-Si symmetric dimer. This large energy gain prevents the Ge-up/Si-down asymmetric dimer from flipping to a Ge-down/Si-up dimer. Therefore, Ge deposition anchored the asymmetric dimers at their adsorbed sites. The energetically stable Ge-Si asymmetric dimer fixes the flip-flop motion of the adjacent Si-Si dimers. The fixed Si-Si asymmetric dimer also halts the flip-flop motion of their adjacent dimers. Freezing of the flip-flop motion propagates along the dimer rows in this manner. We presume that this is why a small amount of Ge atoms made all the surface dimers buckle, even though the Ge atoms could not cover all the surface sites.

The STM image of asymmetric dimers at $\theta_{Ge} = 0.56$ ML is consistent with the theoretical calculations indicating that the surface tends to accept Ge-up/Si-down asymmetric

dimers at $\theta_{Ge} = 0.50$ ML.^{26,27} The calculations also verified that $c(2 \times 4)$ and $p(2 \times 2)$ are not energetically different at the Ge/Si(001) surface at $\theta_{Ge} = 0.50$ ML. The asymmetric dimers seemed to have no preference in taking $c(2 \times 4)$ and $p(2 \times 2)$ local ordering at 0.28 and 0.56 ML, as the theory predicted. However, the experimental results indicated that the asymmetric dimers favor $c(2 \times 4)$ local ordering at larger Ge coverage. While no theoretical preference of $c(2 \times 4)$ and $p(2 \times 2)$ local ordering at larger coverages has been reported, a preference for $c(2 \times 4)$ ordering with θ_{Ge} seemed obvious.

DVLs appeared at $\theta_{Ge} \geq 0.5$ ML. The DVL's are introduced to reduce the outward expansion with Ge deposition by creating a trench of missing dimer lines. However, the formation of missing dimers consumes energy. A balance between the Ge-induced strain and dimer vacancy formation energy determines the distance between DVLs (N).^{16,17} The accumulation of the strain could be partially relaxed here by mixing Ge and Si atoms in the top surface and subsurface layers. Thus, the intermixing can be estimated from the θ_{Ge} -dependence curve of N . Voightlander and Kastner reported a θ_{Ge} dependence of N in a case without mixing. They also showed N at $\theta_{Ge} = 2.0$ ML in 25% and 12% mixing cases.¹⁶ These are indicated by a dashed line, a square, and a diamond in Fig. 2. The figure suggests that $\sim 10\%$ of the deposited Ge atoms diffused into the Si subsurface layer while $\sim 90\%$ of the Ge atoms remained at the top surface layer during growth at 680 °C.

The above estimation indicates that the top layer consisted primarily of Ge atoms resting on a Si subsurface layer at $\theta_{Ge} = 1.12$ ML. Jenkins and Srivastava demonstrated theoretically²⁶ that the Ge-Ge buckled dimer structure is energetically most favorable at a full monolayer Ge/Si(001) surface. Thus, the zigzag chains on a 1.12 ML surface are mainly due to asymmetric Ge-Ge dimers standing on a Si subsurface layer. However, Jenkins and Srivastava also estimated that 11% of Ge atoms occupy a metastable subsurface site at 1000 K based on the energy difference between a Ge-Ge buckled dimer and dimers in which Ge atoms occupy subsurface sites. This estimate is consistent with our estimate above. Furthermore, the calculation demonstrates that the dimers standing on Ge atoms in the subsurface layer also favor an asymmetric dimer structure. Thus, it is reasonable for a surface $\theta_{Ge} = 1.12$ ML grown at 680 °C to assume an asymmetric dimer structure everywhere, irrespective of 10% diffusion of Ge to the subsurface layer.

Symmetric dimer domains reappeared locally at $\theta_{Ge} = 1.68$ ML. The disappearance of local symmetric dimer domains at liquid N₂ temperature demonstrates that the symmetric dimer domains are due to the thermally activated flip-flop motion of asymmetric dimers frozen at low temperatures. At 1.68 ML, Ge-Ge dimers are regarded to be on the subsurface layer, $\sim 50\%$ of which are occupied by Ge atoms. Meanwhile, the symmetric dimer domains represented $\sim 20\%$ of the overall surface at $\theta_{Ge} = 1.68$ ML. Thus, the symmetric dimer domains were not directly related to the Ge-Ge dimers on the Ge subsurface. Instead, we suggest stress-domain formation at Ge(001) surfaces of a few

defects¹¹ as the cause of the reappearance of the symmetric dimer domains. Although the initial Si(001) surface included many defects, the DVLs gettered the defects at Ge/Si(001) surfaces. The defect density reduced dramatically at the surface of $\theta_{Ge} = 1.68$ ML. Thus, stress-domain formation may be possible on the surface of $\theta_{Ge} = 1.68$ ML as well as on the Ge(001) surfaces of a few defects. $c(2 \times 4)$ and 2×1 domains alternated along the dimer bond direction at the Ge(001) surface. A first principles calculation²⁸ suggested that $c(2 \times 4)$ and 2×1 domains have different anisotropic tensile stresses along their dimer bond. The coexistence of $c(2 \times 4)$ and 2×1 domains totally relaxes the anisotropic stress at the surface at a cost of domain wall formation.^{11,29} Although $c(2 \times 4)$ and 2×1 domains did not appear periodically at the Ge/Si(001) surface of $\theta_{Ge} = 1.68$ ML, the coexistence of $c(2 \times 4)$ and 2×1 domains is also regarded to relax the stress along the dimer bond.

The surface of $\theta_{Ge} = 1.12$ ML with $c(2 \times 4)$ domains is also expected to favor the coexistence of $c(2 \times 4)$ and 2×1 domains to relax the anisotropic stress along the dimer bond. However, the surface took on $c(2 \times 4)$ local ordering only at $\theta_{Ge} = 1.12$ ML. We suppose that θ_{Ge} -dependent reduction of the potential barrier of the flip-flop motion of the asymmetric dimers explains why the 2×1 appeared at $\theta_{Ge} = 1.68$ ML but not at 1.12 ML. Miwa demonstrated theoretically that a Ge-Si mixed asymmetric dimer is energetically 0.55 eV more stable than a symmetric dimer, while a Ge-Ge asymmetric dimer is 0.30 eV more stable than a Ge-Ge symmetric dimer.²⁷ These calculations suggest a trend of barrier reduction with θ_{Ge} , although no estimate was published for the Ge-Ge dimer on a Ge-Si mixed subsurface layer. This suggests that the barrier was high enough at $\theta_{Ge} = 1.12$ ML to quench the flip-flop motion and block the appearance of 2×1 domains. However, if the barrier is reduced, 2×1 domains could reappear to relax the anisotropic stress at $\theta_{Ge} = 1.68$ ML.

Finally, we will discuss the interaction of asymmetric dimers with DVLs. The second-layer atoms rebond to make dimers at DVLs and reduce the energy cost of dangling bonds.¹⁷ The resulting structures are shown by a ball-and-stick model in Figs. 4(b) and 4(c). The second-layer atoms in the DVL are indicated by black dots in the models. The line between two black dots in the DVL is a dimer formed between the two second-layer atoms. The upper and lower atoms of the buckled dimers are indicated by large shaded and open circles in the upper and lower domains. The upper and

lower atoms of asymmetric dimers dehybridize their back-bond sp^3 orbitals to make sp^2 -like and p -like orbitals in the buckled dimer structure.²⁷ This causes local compressive (tensile) stresses on the second-layer atoms under the upper (lower) atoms of the top surface asymmetric dimers. The directions of these stresses on the second-layer atoms in the DVL are indicated by arrows in Figs. 4(b) and 4(c). The second-layer atoms paired by dimers in the DVL experience stress of the same direction when the upper atoms of the asymmetric dimer in the upper domain face the lower atoms of the dimer in the lower domain in the model, as shown in Fig. 4 (b). However, the paired second-layer atoms undergo stresses of opposite directions, breaking up the dimer at an upper atom site and compressing the dimer at a lower atom site in the DVL if the upper atoms in the upper domain face the lower atoms in the lower domain [Fig. 4(c)]. Thus, model (b) is energetically favorable over model (c). We assume that this is the reason for the phase inversion of zigzag chains at the DVLs. The zigzag chains in the upper domain correlate to those in the lower domain due to the dimers in the DVLs so as to reverse the zigzag phase at the DVL. The flip-flop of asymmetric dimers in the upper domain is transferred to the dimer rows in the lower domain facing the DVL by maintaining this correlation. This causes the 2×1 domains to extend along the dimer row direction over the DVL.

V. SUMMARY

In summary, we studied the evolution of a dimer structure on a Ge/Si(001) surface with Ge coverage. A small amount of Ge completely changed the symmetric dimers of the Si(001) surface to asymmetric dimers. DVLs were introduced to the surfaces at $\theta_{Ge} \geq \sim 0.5$ ML. High-resolution STM images indicated that the phase of the buckled dimer alternation inverted at the DVL. Dimerization of the second-layer atoms in the DVL causes phase inversion of the buckled dimer alternation at the DVL. Here 2×1 domains with symmetric dimers reappeared with further deposition. Low-temperature STM indicated that the symmetric dimers are due to the flip-flop motion of buckled dimers reactivated at room temperature. Reduction of the potential barrier of the flip-flop motion of asymmetric dimers enabled the reappearance of the 2×1 domain at $\theta_{Ge} = 1.68$ ML. The anisotropic stress along the dimer bond was relaxed by introducing 2×1 domains into $c(2 \times 4)$ domains. The phase correlation over the DVL made the 2×1 domains of flip-flopping asymmetric dimers extend along the dimer rows over the DVL.

*Corresponding author. Electronic address: hirayama@materia.titech.ac.jp

¹J. Dabrowski and H-J. M-sig, *Silicon Surface and Formation of Interfaces* (World Scientific, River Edge, NJ, 2000).

²H.J.W. Zandvliet, *Rev. Mod. Phys.* **72**, 593 (2000).

³R.J. Hamers and U. Kohler, *J. Vac. Sci. Technol. A* **7**, 2854 (1989).

⁴R.M. Tromp, R.J. Hamers, and J.E. Demuth, *Phys. Rev. Lett.* **55**, 1303 (1985).

⁵R.J. Hamers, R.M. Tromp, and J.E. Demuth, *Phys. Rev. B* **34**, 5343 (1986).

⁶J. Ihm, M.L. Cohen, and D.J. Chadi, *Phys. Rev. B* **21**, 4592 (1980).

⁷R.A. Wolkow *Phys. Rev. Lett.* **68**, 2636 (1992).

⁸M. Kubota and Y. Murata, *Phys. Rev. B* **49**, 4810 (1994).

⁹J.A. Kubby, J.E. Griffith, R.S. Becker, and J.S. Vickers, *Phys. Rev. B* **36**, 6079 (1987).

¹⁰J.A. Kubby and J.J. Boland, *Surf. Sci. Rep.* **26**, 61 (1996).

¹¹H.J.W. Zandvliet, B.S. Swartzentruber, W. Wulfhekkel, B.J. Hat-tink, and B. Poelsema, *Phys. Rev. B* **57**, R6803 (1998).

¹²T.I. Kamins, G. Medeiros-Ribeiro, D.A.A. Ohlberg, and R.S. Williams, *J. Appl. Phys.* **85**, 1159 (1999).

- ¹³G. Wedler, J. Walz, T. Hesjedal, E. Chilla, and R. Koch, Phys. Rev. Lett. **80**, 2382 (1998).
- ¹⁴M. Kastner and B. Voigtlander, Phys. Rev. Lett. **82**, 2745 (1999).
- ¹⁵X. Chen, F. Wu, Z. Zhang, and M.G. Lagally, Phys. Rev. Lett. **73**, 850 (1994).
- ¹⁶B. Voigtlander and M. Kastner, Phys. Rev. B **60**, R5121 (1999).
- ¹⁷J. Tersoff, Phys. Rev. B **45**, 8833 (1992).
- ¹⁸F. Wu, X. Chen, Z. Zhang, and M.G. Lagally, Phys. Rev. Lett. **74**, 574 (1995).
- ¹⁹F. Wu and M.G. Lagally, Phys. Rev. Lett. **75**, 2534 (1995).
- ²⁰M. Kummer, B. Vogeli, T. Meyer, and H. von Kanel, Phys. Rev. Lett. **84**, 107 (2000).
- ²¹S.-J. Kahng, Y.-J. Park, and Y. Kuk, Surf. Sci. **440**, 351 (1999).
- ²²F. Iwawaki, M. Tomitori, and O. Nishikawa, Ultramicroscopy **42-44**, 902 (1992).
- ²³H. Tochihara, T. Sato, T. Sueyoshi, T. Amakusa, and M. Iwatsuki, Phys. Rev. B **53**, 7863 (1996).
- ²⁴F. Iwawaki, M. Tomitori, and O. Nishikawa, Surf. Sci. **266**, 285 (1992).
- ²⁵X. Chen, D.K. Saldin, E.L. Bullock, L. Patthey, L.S.O. Johansson, J. Tani, T. Abukawa, and S. Kono, Phys. Rev. B **B55**, R7319 (1997).
- ²⁶S.J. Jenkins and G.P. Srivastava, Surf. Sci. **377**, 887 (1997).
- ²⁷R.H. Miwa Surf. Sci. **418**, 55 (1998).
- ²⁸R.A. Garcia and J.E. Northrup, Phys. Rev. B **B48**, 17 350 (1993).
- ²⁹O.L. Alerhand, D. Vanderbilt, R.D. Meade, and J.D. Joannopoulos, Phys. Rev. Lett. **61**, 1973 (1988).